
This is an electronic reprint of the original article.
This reprint may differ from the original in pagination and typographic detail.

Yang, X.; Tian, Y.; Schicker, I.; Jung, A.

Wind to start the washing machine? High-Resolution Wind Atlas for Finland

Published in:
arXiv.org

Accepted/In press: 01/03/2023

Please cite the original version:

Yang, X., Tian, Y., Schicker, I., & Jung, A. (in press). Wind to start the washing machine? High-Resolution Wind Atlas for Finland. *arXiv.org*. <https://arxiv.org/abs/2303.04403>

This material is protected by copyright and other intellectual property rights, and duplication or sale of all or part of any of the repository collections is not permitted, except that material may be duplicated by you for your research use or educational purposes in electronic or print form. You must obtain permission for any other use. Electronic or print copies may not be offered, whether for sale or otherwise to anyone who is not an authorised user.

Wind to start the washing machine?

High-Resolution Wind Atlas for Finland

1st Xu Yang

Dept. of Computer Science
Aalto University
Espoo, Finland
xu.l.yang@aalto.fi

2nd Yu Tian

Dept. of Computer Science
Aalto University
Helsinki, Finland
yu.tian@aalto.fi

3rd Irene Schicker

Dept. of Postprocessing
GeoSphere Austria
Vienna, Austria
irene.schicker@geosphere.at

4th Alexander Jung

Dept. of Computer Science
Aalto University
Helsinki, Finland
alex.jung@aalto.fi

Abstract—The current fossil fuel and climate crisis has led to an increased demand for renewable energy sources, such as wind power. In northern Europe, the efficient use of wind power is crucial for achieving carbon neutrality. To assess the potential of wind energy for private households in Finland, we have conducted a high spatiotemporal resolution analysis. Our main contribution is a wind power map of Finland that indicates the availability of wind power for given load profiles. As a representative example of power load, we consider the load profile of a household appliance. We compare this load profile against the wind power available nearby the weather stations of the Finnish meteorological institute.

Index Terms—fossil fuel free, renewable, wind energy, exploratory data analysis, smart grid

I. INTRODUCTION

The efficient use of renewable energy is a key component for the green transition of current fossil-fuel based industries to achieve carbon neutrality [1]. Wind energy is a main source for renewable energy in Nordic countries such as Finland, especially during winter months [2]. According to the up-to-date statistics(2022), wind power has covered 14,1% of the Finnish electricity consumption [3].

A key challenge in the efficiently using of wind energy is its spatio-temporal variability. In general, wind energy is available at locations and during times, which may not always match the end-user's needs (household appliance). The transfer of wind energy across space and time requires well-designed power grids and efficient storage facilities such as batteries [4, 5].

Since the transmission of wind energy incurs losses [6], it is beneficial to consume the wind energy near its production sites. This highlights the importance of site selection for wind power plants, which often requires corresponding estimation of wind production. Previous studies [7]–[10] have found that Weibull distribution is a useful tool for the evaluation of wind resources for chosen sites, due to its ability to properly fit wind data as a probability distribution function.

Historical wind speed observation data of Malaysia has been used to evaluate wind power density and inform wind power plant site selection in [11]. The authors of [12] combined geographic information systems with multi-criteria decision making to optimize the site selection in Thailand. These works use a long-term average perspective, based on the statistics of wind speed and power production. In contrast, we are

interested in the short-term availability of wind power to operate household appliances, equipped with modest battery capacity.

Our work is most closely related to recent efforts in generating various instances of a wind power atlas [13, 14]. In particular, the NEWA and ERA5 reanalysis data sets have been proposed for wind analysis fields with a temporal resolution of 30 and 60 minute intervals, respectively, and spatial resolutions of 3 and 30 km, respectively. In contrast to these existing works, our approach uses a higher temporal resolution with 10 minute intervals. On the other hand, our approach focuses on local wind power generation dictated by the locations of weather stations operated by the Finnish Meteorological Institute (FMI).

Contribution. This paper provides the results of an exploratory data analysis using freely available weather data provided by FMI. The aim of this analysis is to generate a high-resolution wind-power map for Finland. For each FMI station we determine the fraction of the year 2021 during which an appliance with a given power profile could be powered solely from wind power.

Notation. We denote the first n natural numbers starting with 0 as $[n] := \{0, \dots, n-1\}$. V for wind speed, P for wind power, and E for energy are used throughout the paper. Other symbols are defined as required.

II. PROBLEM SETTING

We consider the simple power system depicted in Figure 1 during discrete time instants $t = 0, 1, \dots$. The absolute time difference between any two consecutive time instants t and $t+1$ is $\Delta t = 10\text{min}$. The system includes a wind power plant that delivers the power $P_t^{(w)}$ at time instant t . We consider a wind power plant of type Nordex N100/25000 https://www.thewindpower.net/turbine_en_224_nordex_n100-2500.php that is mounted at a height of 100 m.

The system in Figure 1 also includes a load that is characterized by a power profile $P_{t'}^{(a)}$ for time instants $t' \in [T_a]$. The total duration (in absolute time) of the load profile is $T_a \cdot 1\text{min}$. An example for the load is a household appliance

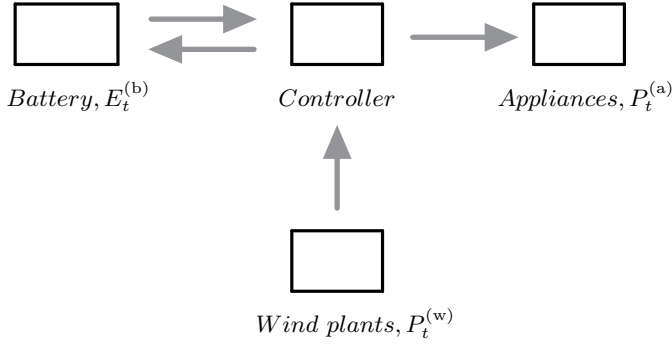


Fig. 1: A wind power plant generates the power $P_t^{(w)}$ at discrete-time t which is used to serve a load with prescribed power profile $P_t^{(a)}$. The surplus (if any) power is used to load a battery whose energy level is $E_t^{(b)}$.

such as a dishwasher or washing machine (see Figure 2). The power profile of the load has finite support of T_a time instants,

$$P_{t'}^{(a)} = 0 \text{ for } t' \notin \{0, 1, \dots, T_a\}.$$

Consider some candidate time instant $t_s \in [365 \cdot 24 \cdot 6]$ during the year 2021. Starting at t_s we try to run the load $P_t^{(a)}$. We assume the battery is empty when starting the load and ignore any power leakage,

$$\begin{aligned} E_{t_s}^{(b)} &= 0, \\ E_{t+1}^{(b)} &= \min \{E_t^{(b)} + (P_t^{(w)} - P_{t-t_s}^{(a)})\Delta t, E_{bat}\} \text{ for } t > t_s. \end{aligned} \quad (1)$$

We define the candidate starting time t_s as **suitable** if $E_t^{(b)} \geq 0$ for $t \in \{t_s, t_s + 1, \dots, t_s + T_a\}$. The useful annual fraction of the year 2021 is defined as

$$\rho := \frac{|\{t_s \in [365 \cdot 24 \cdot 6] : t_s \text{ is suitable}\}|}{365 \cdot 24 \cdot 6} \quad (2)$$

Note that the fraction ρ depends on the battery capacity E_{bat} , the load profile $P_t^{(a)}$ and the available wind power $P_t^{(w)}$. Section III discusses different choices for the battery capacity E_{bat} and load profiles $P_t^{(a)}$ that are used to determine the useful annual fractions $\rho^{(i)}$ nearby FMI weather stations, indexed by $i \in \{1, 2, \dots\}$.

III. METHOD

To determine the useful fractions $\rho^{(i)}$ nearby FMI station $i = 1, 2, \dots$, we estimate the available wind power from the wind speed observations at a height of 10 m. Section III-A explains the pre-processing of raw weather observations, including the imputation of missing observations, extrapolation of wind speed at 10 m to 100 m, and the estimation of wind power generation at 100 m. Section III-B discusses representative power load profiles that we will use for computing the useful fractions and generating the wind power atlas.

A. Pre-Processing Wind Observations

We downloaded wind speed observations V_t (height = 10 m) at time instants $t = \{0, 1, \dots, 365 \cdot 24 \cdot 6\}$ during year 2021 at different FMI stations from the web interface <https://en.ilmatiteenlaitos.fi/open-data>. In a next step we excluded any weather station for which more than 3% wind observations were missing. The resulting 165 FMI weather stations, indexed $i = 1, 2, \dots, 165$, are then used to construct the wind atlas in Section IV.

Data Imputation. For some weather stations, the wind speed observations are missing (we also treat negative wind speed values as missing values) at some time instants. We choose to impute missing wind observations via linear temporal interpolation [15]. If we denote t_m and t_n the time instants just before and after the time instants of missing observations,

$$\hat{V}_t = \frac{V_{t_m} - V_{t_n}}{t_m - t_n} \cdot (t - t_m) + V_{t_m} \text{ for } t \in \{t_m + 1, \dots, t_n - 1\}. \quad (3)$$

From Wind Speed to Wind Power: We use the “1/7 wind power law” [16] to extrapolate the wind speed measured at the height of 10 m to the expected wind speed at 100 m (the wind turbine hub height):

$$\hat{V}_{100} = V_{10} \cdot \left(\frac{100}{10}\right)^\alpha \quad (4)$$

with

$$\alpha = 1/7.$$

The estimated wind speed \hat{V}_{100} at each time instant t is then combined with the power curve of the turbine Nordex N100/25000 to obtain an estimate for the generated power $P_t^{(w)}$. In particular, the estimated power \hat{P} delivered by the turbine for an estimated wind speed in the range $V_j < \hat{V}_{100} < V_{j'}$ is

$$\hat{P} = \frac{P_j - P_{j'}}{V_j - V_{j'}} \cdot (\hat{V}_{100} - V_j) + P_j \quad (5)$$

Here, P_j and $P_{j'}$ denote, respectively, the nominal wind power delivered at wind speeds V_j and $V_{j'}$.

B. Power Load Profiles

We use the open dataset <https://www.kaggle.com/datasets/uciml/electric-power-consumption-data-set> to construct two prototype load profiles $P_t^{(a)}$. The first load profile $P_t^{(dw)}$ corresponds to a single dishwasher. The second load profile $P_t^{(house)}$ represents an entire single-family household.

Single Appliance. We extracted the load power profile $P_t^{(dw)}$ (Figure 2) of a dishwasher from the dataset [17].

The overall duration of the dishwasher process is 75 minutes with time intervals of 1 minute. To align the different time intervals of dishwasher load profile and wind speed records from FMI, wind speed is assumed to be constant during each 10 min time interval. Based on this assumption, we implemented (1) on a 1-min interval to run the corresponding numerical experiments.

Entire Household. Figure 3 depicts a representative load profile $P_t^{(house)}$ for a private household during an entire day

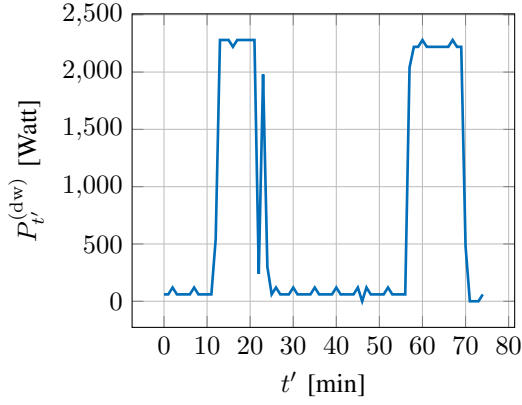


Fig. 2: The load profile of a dishwasher with time intervals of 1 minute.

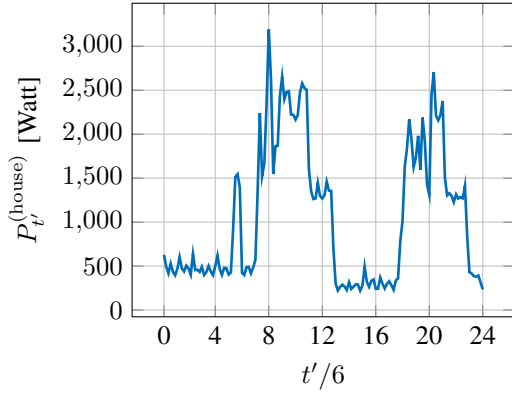


Fig. 3: Load profile of a representative household during an entire day which corresponds to a duration of $T_a = 24 \cdot 6$ time instants (10 minute intervals).

[17]. The duration of the profile $P_{t'}^{(house)}$ is $T_a = 24 \cdot 6$ time instants.

IV. WIND POWER ATLAS FOR FINLAND

Numerical experiments were then conducted to explore fine-resolution temporal and spatial variations of the wind power resource in Finland via virtually running this dishwasher process according to Eq. (1) and Eq. (2). Table I shows useful annual fractions at FMI weather stations, given different battery capacities. The useful fractions increase as the battery capacity increases until a certain value (between 800 and 1000Wh) is reached. Increasing battery capacity beyond this value has no effect on the resulting useful annual fractions.

Figure 4 is a map of Finland, in the location of FMI weather station i , a red dot is added as a marker; the marker size represents the corresponding useful annual fraction $\rho^{(i)}$. The map clearly indicates that wind power has a high availability in regions along the coastline and in the northern parts of Finland.

We also did further analysis to explore the periodic variation of useful fractions over 24 hours of the day and 12 months of the year. Figure 6 shows an example weather station

TABLE I: Summary statistics for the useful fraction of 2021 to run a dishwasher (see Figure 2) only with wind power.

Battery capacity	Min fraction	Max fraction	Mean	std
200Wh	0.14	0.96	0.66	0.19
500Wh	0.18	0.97	0.70	0.18
800Wh	0.20	0.97	0.72	0.18
1000Wh	0.21	0.97	0.72	0.17
1500Wh	0.21	0.97	0.72	0.17
2000Wh	0.21	0.97	0.72	0.17

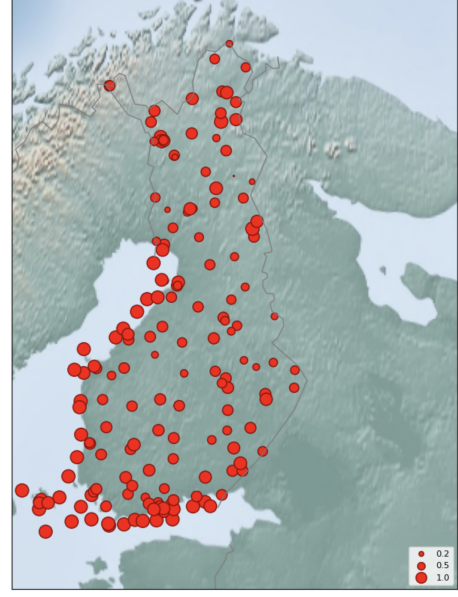


Fig. 4: Spatial distribution of useful annual fractions $\rho^{(i)}$ of 2021 during which the load profile $P_{t'}^{(dw)}$ (see Figure 2) could have been powered only from wind power (using a battery capacity $E_{bat} = 1000\text{Wh}$). Each dot represents an FMI weather station, indexed by $i = 1, \dots, 165$ and its radius is scaled by $\rho^{(i)}$.

Sotkamo Tuhkakyla where useful annual fraction is 0.7, but the distribution over 24 hours is quite uniform. To quantize the uniformity of the distribution for each station, information entropy is applied; in particular, the following formula is used to calculate the entropy

$$H = - \sum_{i=1}^{24} p_i \log p_i$$

where p_i is the fraction of useful starting time points that fall into the i th hour of a day during 2021.

The result shows the entropies for all weather stations included in this study are larger than 0.97, indicating the distribution of useful starting time points is quite uniform over the 24 hours of a day.

Whereas the distribution characteristic over 12 months of the year is different. Figure 5 (a, b, c) show significant seasonal trends in some weather stations, and the trends match the general characteristics of wind speed in Finland:

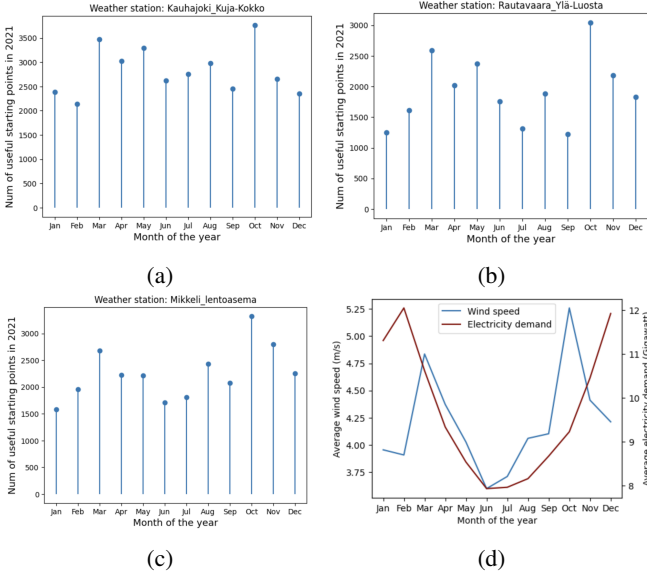


Fig. 5: Distribution of useful starting points over 12 months at some weather stations (plots a,b,c) and a comparison between average wind speed and electricity demand of year 2021 (plot d)

average wind speed of March and October is relatively higher (year 2021)(Figure 5 (d)). A further comparison with the trend of electricity demand in Finland (year 2021) shows during the summer months (June, July, and August), lower electricity demand is aligned with lower wind speed, but the trend is not quite consistent during winter months when the electricity demand achieves peaks. Electricity demand data is from FinGrid open database [18].

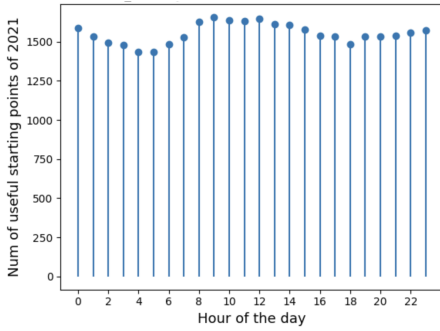


Fig. 6: Distribution of useful starting points over 24h in Sotkamo Tuhkakyla weather station.

From Table II, we can see compared to running a dishwasher, larger battery capacity is needed to fully exploit the wind resources to provide power for an entire house with profile $P_{t'}^{(\text{house})}$. Similarly, a map (Figure 7) is generated to visualise the useful annual fractions of 2021.

Comparison with NEWA and ERA5. While wind speeds observations from FMI have a high temporal resolution (10-min intervals), they only allow for a poor spatial resolution of the resulting wind power atlas. Some sites are quite close

TABLE II: Useful annual fractions in FMI weather stations to provide wind power for an entire house, given different battery capacities.

Battery capacity	Min fraction	Max fraction	Mean	std
1000Wh	0.17	0.97	0.68	0.18
1500Wh	0.19	0.97	0.70	0.18
2000Wh	0.19	0.97	0.71	0.18
2500Wh	0.20	0.97	0.72	0.17
3000Wh	0.20	0.97	0.72	0.17

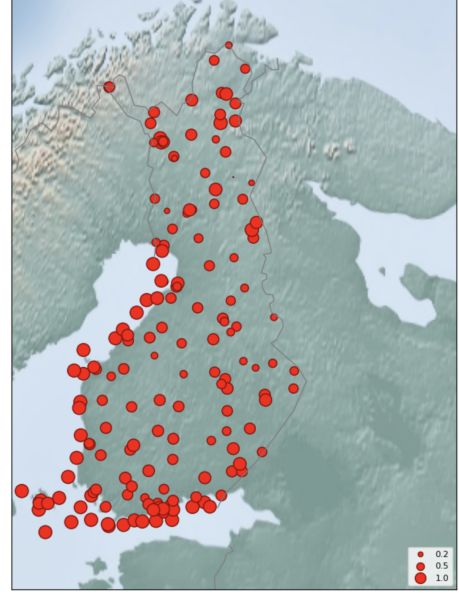


Fig. 7: Spatial distribution of annual useful fractions $\rho^{(i)}$ of 2021 during which the load profile $P_{t'}^{(\text{house})}$ (see Figure 3) could have been powered only from wind power (using a battery capacity $E_{bat} = 2500\text{Wh}$). The markers (red dots) represents FMI weather stations, indexed by $i = 1, \dots, 165$. The marker size (radius) is scaled by $\rho^{(i)}$.

to each other, with distances less than 1km, and some sites are far away from their neighbors, with distances larger than 50km, though generally, the sites are well distributed. Thus, the wind atlas in Figure 4 and 7 are mostly useful for wind turbine locations nearby FMI weather stations. One possible extension of our approach would be to use high-resolution wind reanalysis data sets to interpolate between FMI weather stations. To this end, we compared FMI observation with reanalysis datasets from NEWA [13] and ERA5 [14], which use the Weather Research and Forecasting Model (WRF) and the European Centre for Medium-Range Weather Forecasts Integrated Forecasting System (ECMWF-IFS), respectively. As NEWA only updated the reanalysis dataset to the year 2018, so we also downloaded corresponding data of the year 2018 from FMI for comparison. From Figure 8 and 9, we can see NEWA data and ERA5 data generally compare well to FMI observations except for some northern FMI stations of Finland.

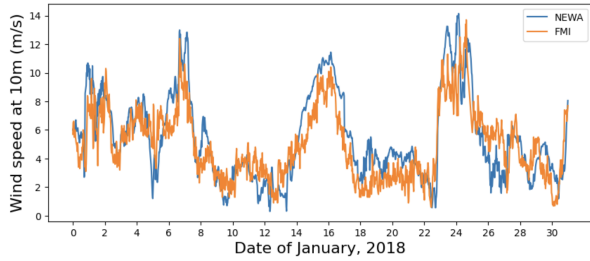


Fig. 8: Comparing modelled wind speed from NEWA with FMI wind speed observations during Year 2018 at Helsinki Kumpula)

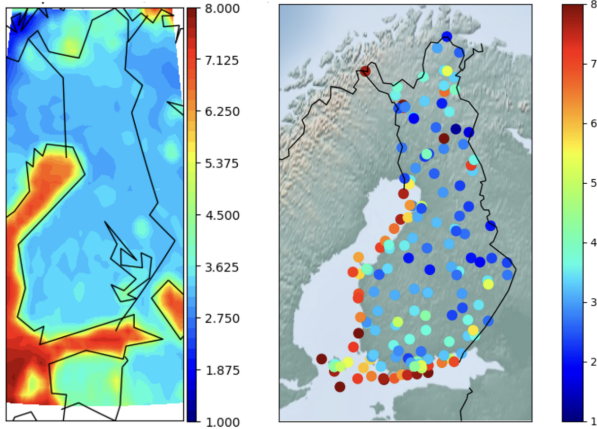


Fig. 9: Left: ERA5 reanalysis data for the average wind speed at 10 m height during year 2021. Right: Dots represent FMI weather stations with dot color represents the average observed wind speed at 10 m height during year 2021.

V. CONCLUSION

We have used open weather data from the FMI to construct a wind power atlas for Finland. Unlike existing approaches for constructing a wind power atlas, our method employed a high temporal resolution that allows to verify whether a particular load profile could be powered solely by a wind turbine (combined with a battery storage capacity). Our results indicate that wind power has a high availability in regions along the coastline and in northern parts of Finland. We highlight that our analysis was exploratory using historical observation data from previous years. As an important next step, we will consider the short-term predictability of wind power in Finland.

REFERENCES

- [1] <https://julkaisut.valtioneuvosto.fi/handle/10024/164323>.
- [2] <https://www.stat.fi/uutinen/energy-in-finland-2022-information-package-on-energy>.
- [3] <https://tuulivoimayhdistys.fi/en/ajankohtaista/statistics/wind-power-statistics-2022>.
- [4] W. Qi, Y. Liang, and Z.-J. M. Shen, "Joint planning of energy storage and transmission for wind energy generation," *Operations Research*, vol. 63, no. 6, pp. 1280–1293, 2015.

- [5] D. Willis, C. Niezrecki, D. Kuchma, E. Hines, S. Arwade, R. Barthelmie, M. DiPaola, P. Drane, C. Hansen, M. Inalpolat *et al.*, "Wind energy research: State-of-the-art and future research directions," *Renewable Energy*, vol. 125, pp. 133–154, 2018.
- [6] J. M. Morales, P. Pinson, and H. Madsen, "A transmission-cost-based model to estimate the amount of market-integrable wind resources," *IEEE Transactions on Power Systems*, vol. 27, no. 2, pp. 1060–1069, 2012.
- [7] P. Wais, "Two and three-parameter weibull distribution in available wind power analysis," *Renewable energy*, vol. 103, pp. 15–29, 2017.
- [8] M. A. Baseer, J. P. Meyer, S. Rehman, and M. M. Alam, "Wind power characteristics of seven data collection sites in jubail, saudi arabia using weibull parameters," *Renewable Energy*, vol. 102, pp. 35–49, 2017.
- [9] A. N. Celik, "A statistical analysis of wind power density based on the weibull and rayleigh models at the southern region of turkey," *Renewable energy*, vol. 29, no. 4, pp. 593–604, 2004.
- [10] A. K. Azad, M. G. Rasul, and T. Yusaf, "Statistical diagnosis of the best weibull methods for wind power assessment for agricultural applications," *Energies*, vol. 7, no. 5, pp. 3056–3085, 2014.
- [11] N. Masseran, A. Razali, and K. Ibrahim, "An analysis of wind power density derived from several wind speed density functions: The regional assessment on wind power in malaysia," *Renewable and Sustainable Energy Reviews*, vol. 16, no. 8, pp. 6476–6487, 2012.
- [12] A. Bennui, P. Rattanamanee, U. Puetpaiboon, P. Phukpattaranont, and K. Chetpattananondh, "Site selection for large wind turbine using gis," in *PSU-UNS international conference on engineering and environment*, 2007, pp. 561–566.
- [13] <https://map.neweuropeanwindatlas.eu/>.
- [14] <https://www.ecmwf.int/en/forecasts/datasets/reanalysis-datasets/era5>.
- [15] C. Federer, C. Vörösmarty, and B. Fekete, "Intercomparison of methods for calculating potential evaporation in regional and global water balance models," *Water Resources Research*, vol. 32, no. 7, pp. 2315–2321, 1996.
- [16] L. J. De Chant, "The venerable 1/7th power law turbulent velocity profile: a classical nonlinear boundary value problem solution and its relationship to stochastic processes," *Applied Mathematics and Computation*, vol. 161, no. 2, pp. 463–474, 2005.
- [17] F. Paganelli, F. Paradiso, S. Turchi, A. Luchetta, P. Castrogiovanni, and D. Giuli, "Appliance recognition in an osgi-based home energy management gateway," *International Journal of Distributed Sensor Networks*, vol. 11, no. 2, p. 937356, 2015.
- [18] <https://data.fingrid.fi/fi/>.